

On the Use of OFDM for beyond 3G Satellite Digital Multimedia Broadcasting

S. Cioni, G.E. Corazza, M. Neri, and A. Vanelli-Coralli

DEIS/ARCES, University of Bologna
Via V. Toffano, 2/2 - 40125 Bologna ITALY
Email: {scioni, gecorazza, mneri, avanelli}@deis.unibo.it

Abstract—The paper considers the application of Orthogonal Frequency Division Multiplexing (OFDM) techniques in the physical layer of a satellite system devoted to the provision of digital multimedia broadcasting (DMB) services, which are presently the focus of extensive research and development endeavors. In particular, the paper demonstrates that the inherently high spectrum efficiency of OFDM can be retained even in unfavorable propagation channels affected by heavy non-linear and linear distortion, respectively introduced by the on-board high power amplifier and by multipath propagation. This encouraging performance is achieved through the proper design and application of coding and pre-distortion techniques, as described in the paper.

Keywords—OFDM, satellite, predistortion, non-linear distortion, 3G, Rice fading channel

I. INTRODUCTION

In all short-medium term business/market forecasts, the efficient provision of digital multimedia broadcasting (DMB) services in mobile systems appears to be of key importance for mobile operators. More precisely, a recent report [1] foresees spending levels for mobile multimedia content in 2006 at around 3.3 billion in Europe alone. To turn these forecasts into reality, several conditions and requirements will have to be fulfilled:

- Multimedia services must be accepted by the end-users, which is related to low traffic fees (ideally comparable to Internet levels), service continuity over nation wide coverage (in line with today's coverage for mobile voice communications), security issues (preventing virus attacks to personal data), tailored content (adapted to mobile environments and devices), and high sound/image quality.
- Major operators must have interest and willingness to produce and aggregate appealing multimedia services, which is in turn related to cost effective content delivery, wide coverage (to maximize audience), protection against unauthorised content sharing, flexible billing system that includes subscription, bundle, pay per use, etcetera.

Several DMB systems are being developed around the world to meet these challenges. Among others, the MAESTRO integrated project [2] is focusing on an architecture based on a satellite broadcast layer to interwork with 3G and

beyond 3G systems, to provide satellite digital multimedia broadcasting (S-DMB) services to handheld and palmtop terminals. The resulting hybrid architecture makes the most out of satellite broadcast and terrestrial point-to-point technology efficiency. In order to enhance the coverage given by the satellite layer in urban and sub-urban environments, we foresee the use of terrestrial repeaters, also known as Intermediate Module Repeaters (IMRs). These are simple and low-cost transparent repeaters, situated over rooftops or co-located with base station sites, which cover built-up areas very effectively, at the expense of introducing a rather large delay spread.

While the initial implementation of the MAESTRO S-DMB concept is based on the use of the W-CMDA standard [3], we are working on the development of a highly efficient air interface adopting orthogonal frequency division multiplexing (OFDM). Notably, OFDM has been the focus of some interest also in 3GPP [4]. OFDM is known to have in general higher spectral efficiency than WCDMA; however, OFDM is also characterized by a rather high peak-to-average power ratio (PAR), which renders it particularly sensitive to non linear distortion as that introduced by the on-board high power amplifier (HPA). Further, the robustness of OFDM in the specific IMR multipath propagation channel is yet to be established and confirmed.

There is therefore a necessity to prove that OFDM is indeed a suitable solution for the air interface of an S-DMB system. The paper is precisely devoted to the design and analysis of suitable countermeasures to linear and non-linear distortions to allow the transfer of information through an OFDM channel with the desired Quality of Service (QoS). In particular, the use of turbo codes with sufficient channel interleaving, along with suitable pre-distortion techniques, is shown to allow transmission with very limited losses with respect to ideal channel conditions. When interleaving becomes insufficient, due to very slow terminal speeds, the losses become more evident and call for the adoption of additional diversity techniques.

II. THE OFDM TRANSMIT-RECEIVE CHAIN

In the following, we describe the OFDM transmit-receive chain, whose block diagrams are depicted in Fig. 1, Fig. 2, and Fig. 3 in a forward link satellite scenario.

A. Transmitter

According to the 3GPP specifications, during each Transmission Time Interval (TTI), N_b information bits are channel coded by either a convolutional or a turbo code. In this work, we analyze the turbo coding option only, as its application is deemed more likely in the S-DMB case. The turbo code consists of a double rate 1/2 binary Recursive Systematic Convolutional (RSC) code, parallel concatenated and punctured to a rate 1/3. The coded sequence is mapped onto a QPSK constellation to produce the complex sequence $\{a_k\}$, which is then processed by the OFDM modulator in blocks of N_{sc} symbols, N_{sc} odd. The OFDM modulator consists of a serial-to-parallel converter, a N -points IDFT (Inverse Discrete Fourier Transform) processor, and a parallel-to-serial converter. The i -th modulated block at the output of the OFDM modulator is

$$z_n^i = \frac{1}{N} \sum_{q=-\frac{N}{2}}^{\frac{N}{2}-1} Z_q^i e^{j2\pi nq/N} \quad n = 0, \dots, N-1 \quad (1)$$

where

$$Z_q^i = \begin{cases} 0 & -\frac{N}{2} \leq q \leq -\frac{N_{sc}+1}{2} \\ a_{iN_{sc} + \frac{N_{sc}-1}{2} + q} & -\frac{N_{sc}-1}{2} \leq q \leq \frac{N_{sc}-1}{2} \\ 0 & \frac{N_{sc}+1}{2} \leq q \leq \frac{N}{2} - 1 \end{cases} \quad (2)$$

The insertion of the trailing zeros in (2), which corresponds to the insertion of guard bands, is necessary to ensure low out-of-band power. Time separation of the OFDM symbols, necessary to counteract the energy dispersal induced by the multi-path channel, is obtained by the insertion of a cyclic prefix of N_{GS} guard symbols at the output the OFDM modulator, i.e., by feeding the root-raised cosine pulse-shaping filter, with the $N_t = (N + N_{GS} - 1)$ symbols

$$x_k^i = \begin{cases} z_{k+N-N_{GS}}^i & 0 \leq k \leq N_{GS} - 1 \\ z_{k-N_{GS}}^i & N_{GS} \leq k \leq N_t \end{cases} \quad (3)$$

Hence, the complex envelope of the modulated signal is

$$x(t) = \sum_{i=-\infty}^{\infty} \sum_{k=0}^{N_t} x_k^i g(t - kT - iN_t T) \quad (4)$$

where $g(t)$ is the pulse-shaping filter impulse response and T is the sampling time. Interestingly, the parameters N , N_{sc} , N_{GS} , and T influence system performance, complexity and spectral efficiency. According to the 3GPP feasibility study [4], in this work we consider two different sets of parameters: *Set-1* which corresponds to a 512 points IDFT and *Set-2* which corresponds to a 1024 points IDFT. The complete list of parameters for these two sets is reported in Table I.

To cope with the non-linearity due to the on-board HPA, a purposely designed predistortion technique is envisaged in the gateway architecture. In particular, we consider a fractional predistortion technique, based on a Look-Up-Table (LUT) approach, which operates after the shaping filter [6], [7]. The fractional predistorter, acting on the samples, is able to

compensate for the constellation warping due to the phase distortion introduced by the AM/PM HPA characteristic and to reduce the variance of clusters of constellation points, bounding the effects of the inter-symbol interference (ISI). The considered predistorter exploits a linear-in-power indexing strategy, where the table entries are uniformly spaced along the input signal power range, yielding denser table entries for higher amplitudes. It is characterized by a simple implementation, since it requires only a square calculation module, and it is particularly effective if the non-linearities are localized at large amplitudes, which is the case of Travelling Wave Tube (TWT) HPAs. Table entries are computed off-line through the inversion of the HPA characteristics. The first step consists in deriving an analytical model for the HPA. This can be achieved by using an extension of the well-known memoryless Saleh model [8]. The AM/AM and AM/PM TWT HPA characteristics can be expressed by:

$$A[\rho] = \frac{\alpha_a \rho}{\beta_a \rho^2 + 1} \quad (5)$$

$$\Phi[\rho] = \frac{\pi}{3} \frac{\alpha_p \rho^2}{\beta_p \rho^2 + 1} \quad [rad] \quad (6)$$

where $\alpha_a, \alpha_p, \beta_a, \beta_p$ are constant coefficients, and the subscripts a and p denote amplitude and phase, respectively. These coefficients are to be optimized so as to minimize the minimum mean square error (MMSE) between the model and the measured characteristics. Next, the inversion of the analytical model has to be performed. Given $x(t)$ the modulated signal entering the fractional predistorter, its output can be expressed by means of AM/AM and AM/PM characteristics, in a way analogous to the HPA input-output characterization. In particular, if the input signal is expressed as $x(t) = \rho(t) \exp\{j\theta(t)\}$, the complex envelope of the pre-distorted transmitted signal is given by

$$y(t) = R[\rho(t)] \exp\{j(\theta(t) + \Psi[\rho(t)])\} \quad (7)$$

where $R[\cdot]$ and $\Psi[\cdot]$ are the AM/AM and AM/PM predistorter characteristics, respectively [9]. These characteristics are finally set to the inverted Saleh model, obtained through analytic inversion from the HPA AM/AM and AM/PM characteristics. Typical AM/AM and AM/PM HPA characteristics are reported in Fig. 4 and have been used for simulation purposes.

B. Satellite Channel

Assuming, as customary, an ideal feeder link (i.e., the link between the terrestrial gateway and the satellite), the downlink propagation channel experienced by the OFDM signal is depicted in Fig. 2. In this model linear and non-linear distortions, and fading effects are taken into account. For a transparent repeater, the linear distortion is essentially introduced by the on-board input and output multiplexing filters (IMUX and OMUX), which induce significant ISI, that adds to the residual uncompensated ISI induced by the HPA.

On the user link (i.e., the link between the satellite and the mobile user) the OFDM signal is transmitted through a linear time-variant communication channel, with its low-pass equivalent impulse response described by the following model:

$$\tilde{h}'(\tau, t) = \sum_{i=1}^{N_p} \rho_i(t) e^{j[\theta_i(t) + \omega_{di}t]} \delta(\tau - \tau_i) \quad (8)$$

where N_p is the number of paths and, for the i th path, $\rho_i(t)$ is the fading envelope, $\theta_i(t)$ is the phase shift, ω_{di} is the Doppler frequency shift, τ_i is the delay, and $\delta(x)$ indicates Dirac's delta function. In this work, we focus our attention to the single path case. This assumption is in line with the generally accepted notion that in present satellite environments the direct component is generally strong, and multipath power at resolvable delay is relatively very low and can be neglected with no accuracy loss [10]. However, it is worthwhile noting that in the proposed S-DMB architecture, due to the IMR deployment a multipath propagation similar to that experienced in the terrestrial cellular network may occur [11]. We leave this interesting case to future studies which are ongoing within the IST-MAESTRO project.

Under the assumption of single path propagation, the channel low-pass equivalent impulse response reduces to $\tilde{h}'(\tau, t) = \rho(t) e^{j[\theta_1(t) + \omega_{d1}t]} \delta(\tau - \tau_1)$. The fading envelope ρ is assumed to follow a Rice-LogNormal (RLN) distribution [12] and can be written as

$$\rho(t) = R(t)S(t) \quad (9)$$

where $R(t)$ is a stationary Rice random process accounting for small-scale diffuse multipath fading plus a direct signal component, and $S(t)$ is a stationary lognormal random process modeling large-scale shadowing effects. In general, the coherence time of multipath fading is much shorter than that of shadowing. The two processes are assumed to be statistically independent. The RLN model is quite general as it contains as particular cases, as particular cases Rayleigh-lognormal, Rice, Rayleigh, and lognormal distributions, with variable channel dynamics.

Finally, to cope with the introduced channel correlation, ideal interleaving is assumed leading to independent fading between two consecutive OFDM symbols.

C. Receiver

At the receiver side (Fig. 3), perfect frame synchronization is assumed as well as symbol timing recovery. Thus, the sampling times are $t_k = kT$ and the N_{GS} guard symbols are discarded before performing the DFT transform. Then, the DFT sequence enters a soft demodulator whose output is finally decoded by the log-MAP BCJR algorithm with 8 iterations.

III. SIMULATOR ARCHITECTURE

The communication chain has been implemented using an in-house reconfigurable physical layer simulator, identified as PLASMA (*Physical LAYER Simulator for Adaptive*).

PLASMA has been designed keeping in mind both reconfigurability and computational efficiency, which have been achieved by building a modular simulator, in which the single chain module is a stand-alone entity characterized by its own parameters and operating modes. In addition, each single module exchanges data with the outer environment by means of input and output connections, which are reconfigured through an external XML configuration file at launch-time. Not only is it possible to completely modify the way the modules are interconnected, but it is also possible to modify the modules run order, so as to implement nested cycles to increase flexibility. This architecture, supported by a high throughput computing platform such as CONDOR [13], allows to perform clusters of simulations in a reasonable time, considered the 100+ CPUs available.

IV. NUMERICAL RESULTS AND DISCUSSION

Simulation results are reported for packet size $N_b = 1504$, coding rate 1/3, and QPSK modulation in terms of Packet Error Rate (PER) performance against E_b/N_0 .

Results for the OFDM system over the linear AWGN channel are reported in Fig. 5 along with the W-CDMA waveform performance. The OFDM loss with respect to the W-CDMA curve is of approximately 0.3 dB for Set-2 and 0.5 dB for Set-1, thus the distance between the two sets is contained in 0.2 dB. These losses are not unexpected and are fully justifiable by the energy loss associated to the guard times insertion in the OFDM waveform. This energy loss amounts to

$$E_{loss}[dB] = 10 \cdot \log \frac{N + N_{GS}}{N} \text{ dB} \quad (10)$$

Substituting the values given in Table I, we obtain $E_{loss}[dB] = 0.458$ dB for Set-1 and $E_{loss}[dB] = 0.263$ dB for Set-2 as we found out through simulation. Notably, longer guard times, which yield a larger loss, give a stronger resilience to long delay spreads in multipath fading channels. Furthermore, the use of a larger number of carriers in Set-2 by reducing the carrier spacing reduces the resilience to Doppler offsets produced by the UE movement, and also increase the system complexity. These considerations highlight the need for design trade-offs between guard time, energy loss, number of carriers, complexity and performance when multipath scenarios are considered in a mobile environment.

Fig. 5 also shows the impact of non-linear distortion, for different HPA Input Back Offs (IBO) on the OFDM waveform performance in the case of compensation through the fractional predistortion technique and in the case of no-compensation. The obtained results are definitely encouraging: the loss with respect to the linear AWGN case is of about 0.5 dB in the case of IBO = 3 dB and of about 0.75 dB for IBO = 2 dB, for both sets. An interesting figure to evaluate is the total degradation (TD), which accounts for both the E_b/N_0 loss with respect to the linear AWGN channel and the HPA Output Back Off (OBO) at the operating point. For the

IBO = 3 dB case, the OBO results in 1.25 dB, while for IBO = 2 dB the OBO is 0.74 dB. Although in general the IBO/OBO relationship depends on the signal envelope and thus for a OFDM waveform on the number of carriers, it is reasonable to expect a loose dependence of the IBO/OBO relationship when the number of carriers is sufficiently large as the OFDM envelope rapidly converges to the Gaussian one. Given these considerations, the total degradation amounts to 1.75 dB for the IBO = 3 dB case and to 1.49 dB for the IBO = 2 dB case. Within the considered selection of IBOs, the optimum choice is then 2 dB. In the case of no-compensation, there is an additional loss of 0.45 dB for the 3 dB case, that adds to the increased OBO, which reaches 1.35 dB. Hence, the total degradation is 2.3 dB, which is significantly larger than for the predistorted case, showing the effectiveness of the adopted compensation technique.

Considering now the impact of a flat-fading channel, results for Rice factors, K , of 5 dB and 10 dB are shown in Fig. 6, where a linear channel is assumed. For both sets, the loss is of about 0.2 dB for $K = 10$ dB, and of about 0.5 dB for $K = 5$ dB, with respect to the linear AWGN case.

Finally, in Fig. 7 results for the combined non-linear and Rice channel are depicted. As it can be noted, the losses with respect to the linear AWGN are slightly higher than the sum of the losses due to one of the two factors alone. Again, these losses appear to be set-independent, and are of about 1 dB for $K = 10$ dB and IBO = 2 dB, and of about 1.4 dB for $K = 5$ dB and IBO = 2 dB.

These results can be considered very satisfactory taking into account the large sensitivity of the OFDM waveform to non-linear distortions. The adoption of advanced predistortion techniques and powerful channel codes can be seen as the key for exploiting OFDM advantages also in satellite digital multimedia broadcasting networks.

V. SUMMARY AND CONCLUSIONS

OFDM techniques promise for high spectral efficiency and are being used by several broadcast terrestrial systems and have been considered as a good candidate for the evolution of the 3GPP UMTS air interface. Interestingly, the application of the OFDM technique to the satellite based UMTS network has received no attention as it is deemed that the rather high peak-to-average power ratio would lead to excessive OFDM sensitivity to the non linear distortion introduced by the on-board HPA. Although, this is true for a straightforward implementation, in this paper we have demonstrated that the adoption of ad-hoc predistortion techniques along with turbo coding drastically reduces the effect of the HPA non-linear distortion even when a large number of carriers, e.g. 1024, is used at very low HPA input back-off. Moreover, since the used pre-distortion techniques does not decrease the spectral efficiency of the system, OFDM can be considered as a good candidate also for the capacity enhancement of satellite digital broadcasting networks.

ACKNOWLEDGEMENTS

This work is supported by IST/FP6 integrated project MAESTRO partly funded by the European Commission. The authors would like to thank all MAESTRO partners for their valuable contributions to this study.

REFERENCES

- [1] O. Beauvillain, "Paid content more successful on Mobile than on PC", Jupiter MMXI, 17/01/2002
- [2] N. Chuberre, G.E. Corazza, M.G. Francon, C. Nussli, C. Selier, A. Vanelli-Coralli, P. Vincent, "Satellite Digital Multimedia Broadcasting for 3G and beyond 3G systems", *IST Mobile Summit 2004*, Lyon France, 28-30 June 2004.
- [3] H. Holma, A. Toskala, Anti "WCDMA for UMTS - Radio Access for Third Generation Mobile Communications", Ed. John Wiley & Sons, August 2004.
- [4] 3GPP TR 25.892 "Feasibility Study for OFDM for UTRAN enhancement (Release 6)", June 2004
- [5] 3GPP TS 25.212 v. 4.2.0, "Multiplexing and channel coding (FDD)", September 2001.
- [6] P. Salmi, M. Neri, and G.E. Corazza, "Design and Performance of Predistortion Techniques in Ka-band Satellite Networks", *22th International Communication Satellite Systems Conference (ICSSC)*, AIAA, May 2004.
- [7] P. Salmi, M. Neri, and G.E. Corazza, "Fractional Predistortion Techniques with Robust Modulation Schemes for Fixed and mobile Broadcasting", *13th IST Mobile & Wireless Communications Summit (IST2004)*, June 2004.
- [8] S. Chang, E.J. Powers, "Compensation of nonlinear distortion in RF power amplifiers" *Wiley Encyclopedia of Telecommunications*, Proakis J.J. Ed., pp. 530-538.
- [9] A. Brajal, A. Chouly, "Compensation of nonlinear distortions for orthogonal multicarrier schemes using predistortion" *IEEE Globecom Conference, 1994*, Vol. 3, 28 Nov.-2 Dec. 1994, pp. 1909-1914.
- [10] G.E. Corazza, A. Vanelli-Coralli, R. Pedone, and M. Neri, "Mobile Satellite Channels: Statistical Models and Performance Analysis", in *Signal Processing for Mobile Communications Handbook*, August 2004, CRC press.
- [11] C. Caini, G. E. Corazza "Satellite Downlink Reception through Intermediate Module Repeaters: Power Delay Profile Analysis" *EMPS/ASMS 2004 Conf.*, Noordwijk, The Netherlands, 21-22 Sept. 2004.
- [12] G.E. Corazza, F. Vatalaro, "A Statistical Model for Land Mobile Satellite Channels and Its Application to Nongeostationary Orbit Systems", *IEEE Trans. on Veh. Technol.*, Vol. 43, No.3, pp. 738-742, Aug. 1994.
- [13] <http://www.cs.wisc.edu/condor/>, The Condor Project Homepage

Parameter	Set-1 Values	Set-2 Values
TTI Duration [ms]	2	2
FFT/IFFT points (N)	512	1024
Useful carrier (N_{sc})	299	705
Guard interval (N_{GS})	57	64
OFDM sampling rate [Msymb/s]	7.68	6.528
OFDM symbol per TTI	27	12
OFDM symbol duration [μ s]	74.09	166.67
Sub-carrier separation [KHz]	15	6.375
OFDM bandwidth [MHz]	4.485	4.495

TABLE I

3GPP STUDY CASE SYSTEM PARAMETERS [4].

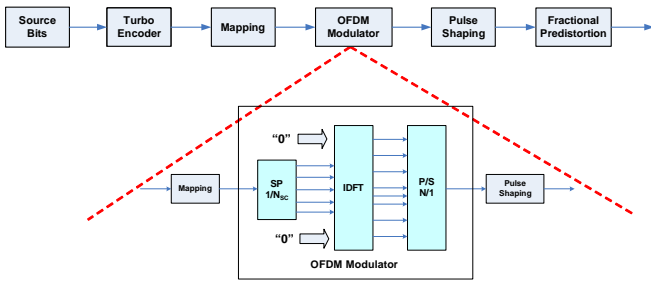


Fig. 1. OFDM Transmitter block diagram.

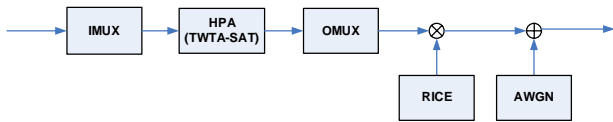


Fig. 2. Channel block diagram.

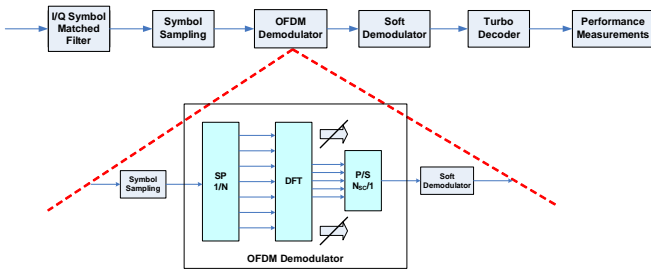


Fig. 3. OFDM Receiver block diagram.

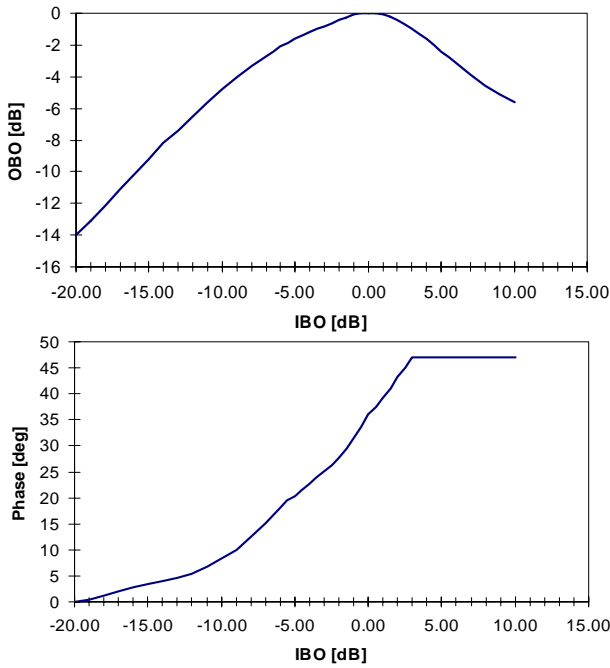


Fig. 4. HPA AM/AM and AM/PM characteristics.

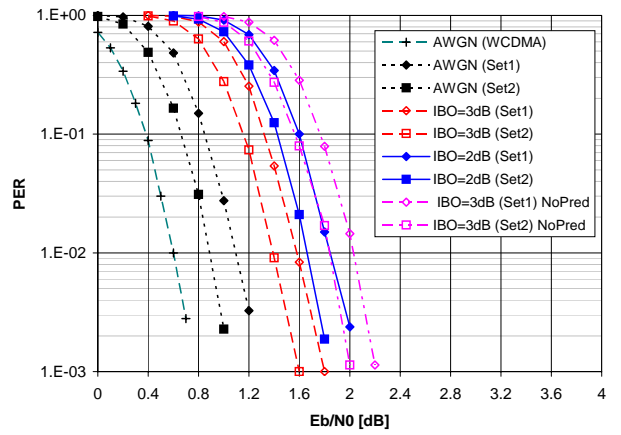


Fig. 5. Rate 1/3 QPSK OFDM system performance considering non-linear distortion, IBO = 2 dB and IBO = 3 dB, AWGN channel. NoPred label corresponds to the no-compensation case.

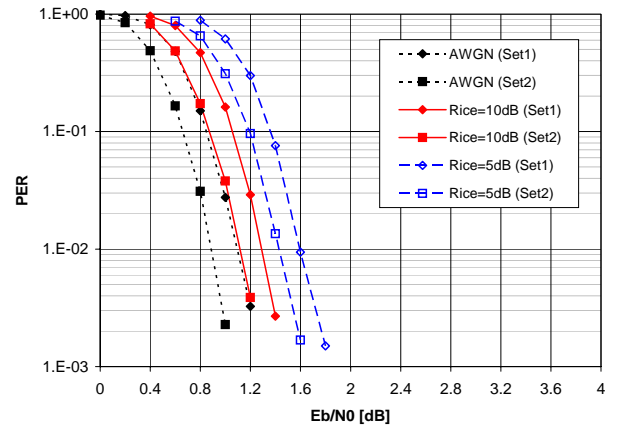


Fig. 6. Rate 1/3 QPSK OFDM system performance over a flat-fading Rice channel with $K = 10$ dB and $K = 5$ dB.

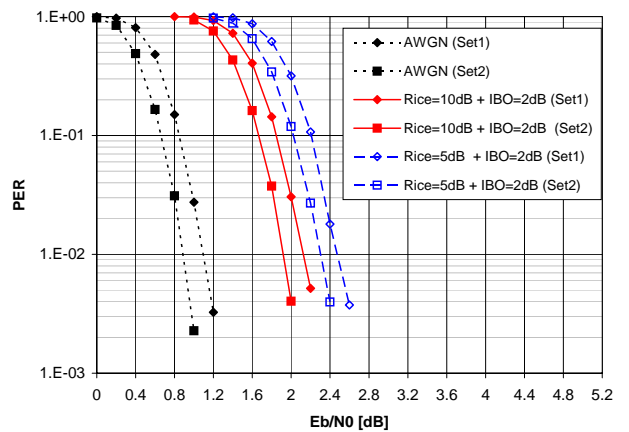


Fig. 7. Rate 1/3 QPSK OFDM system performance over a non-linear flat-fading Rice channel with $K = 10$ dB and $K = 5$ dB, and IBO = 2 dB.